CHEMICAL ROBUSTNESS ENHANCEMENT OF NEGATIVE ELECTRON AFFINITY PHOTOCATHODES THROUGH CESIUM-IODIDE DEPOSITION

S.J. Levenson*, M.B. Andorf, I.V. Bazarov, Q. Zhu, M. Hines, J. Encomendero, D. Jena, V. V. Protasenko, H. G. Xing, and J.M. Maxson, Cornell University, Ithaca, NY, USA A. Galdi, University of Salerno, Fisciano, Italy

Abstract

Photocathodes activated to Negative Electron Affinity (NEA), like GaAs and GaN, allow for efficient production of spin-polarized electrons. Typically activated to NEA with cesium and an oxidant, they are characterized by an extreme sensitivity to chemical poisoning, resulting in a short operational lifetime. In this work, we demonstrate that a cesium iodide (CsI) layer can be used to enhance the dark lifetime of both GaN and GaAs photocathodes activated with cesium. The mechanism behind this improvement is investigated using X-ray Photoelectron Spectrosopy (XPS) and Atomic Force Microscopy (AFM).

INTRODUCTION

Accelerators for high-energy and nuclear physics heavily rely on robust photocathodes capable of sustaining high-average current and spin-polarized functionalities [1–5]. Presently, the only method for generating high current in a photoinjector is a GaAs-based photocathode. GaAs has been used at facilities like MAMI [6] and Jefferson Lab [7], with future facilities such as the EIC [1] and ILC [2] also planning its use. Producing spin-polarized electrons from GaAs involves exciting electrons from the top of the valence band, comprising of degenerate light-hole (LH)/heavy-hole (HH) sub-bands and a split-off (SO) sub-band. Circularly-polarized light excites electrons from the degenerate LH/HH sub-band, preserving the light's angular momentum, leading to excitation from the degenerate $P_{3/2}$ state, resulting in spin-polarized beam generation [8, 9].

To overcome the 4.7 eV workfunction of GaAs, the photocathode is brought to a negative electron affinity (NEA) state, where the surface vacuum energy level is lowered below the conduction band minimum, allowing photoemission of valence band electrons by light with photon energies corresponding to the material's bandgap energy (1.43 eV for GaAs) [10]. NEA is attained by deposition of cesium and an oxidant, such as oxygen or NF₃, onto GaAs. Under this approach, NEA GaAs photocathodes suffer from short operational lifetimes due to the weak adhesion of the NEA activation layer to the surface and its high reactivity to residual gases, necessitating operation in extremely high vacuum (XHV) environments, limiting their use to DC photoinjectors [11, 12].

Extensive research efforts have focused on exploring alternative NEA activation coating layers (such as Cs₃Sb and

CsTe) [13–17] and investigating other bulk materials with spin-polarized capabilities [18, 19] such as GaN [20]. For an overview of spin-polarized electron production at Cornell see MOPR81.

This study investigates the use of Cesium Iodide (CsI) as a way to increase NEA lifetime for both GaAs and GaN photocathodes. Although its high work function excludes its use as an emitter material in photoinjectors, CsI has been shown to effectively serve as an activation layer, reducing the high work function of metal photocathodes [21] and enhancing the performance of carbon fibers for field emission beam production [22].

METHODS

GaAs single crystal (100) wafers p-doped to a carrier concentration of $9 \times 10^{18}~{\rm cm}^{-3}$ were purchased from AXT-Tongmei, Inc. and cut to $1x1~{\rm cm}^2$ samples with a diamond scroll. Chemical etching was performed to remove surface oxidation. This included a de-ionized (DI) water rinse, a 30 second immersion in a 1% HCl solution, and a final rinse with DI water and drying with pure nitrogen.

The GaN sample was grown at Cornell with a Veeco Gen10 molecular beam epitaxy (MBE) system. The growth substrate was a $1x1~\rm cm^2$ GaN template on sapphire, which was ultrasonicated in acetone, methanol, and isopropanol for 10 minutes each, and de-gassed at $200^{\circ} C$ for 7 hours prior to growth. A 1 μm Mg-doped (3 \times $10^{19}~\rm cm^{-3})$ p-GaN layer was epitaxially grown on the substrate using a step-flow growth mode under metal-rich conditions. After growth, the sample was transferred to the Cornell Photoemission Laboratory in a static vacuum suitcase.

Both prepared samples were mounted onto a stainless steel puck. Indium foil was used to increase thermal and electrical contact between the sample and the puck. This assembly was then inserted into a UHV growth chamber with a base pressure of 5×10^{-10} Torr. The chamber features a calibrated quartz micro-balance (QMB), a Cs filament source, a CsI evaporative effusion cell and an electrical feedthrough for biasing the photocathode. The CsI evaporative effusion cell was filled with 99.999% pure CsI metal beads from Sigma-Aldrich Chemical Corporation and outfitted with a shutter mechanism.

Before activation, the sample was annealed at 600°C for 6 hours. NEA activation was then initiated through Cs deposition with the filament source. Throughout the growth process, the quantum efficiency (QE) of the photocathode was monitored with a $10~\mu\text{W}$ 532 nm laser for GaAs or a

^{*} sjl354@cornell.edu

and content from this work may be used under the terms of the CC BY 4.0 licence (© 2024). Any distribution of this work must maintain attribution to the author(s), title of the work, publisher, and DOI

10 µW 265 nm LED for GaN. Cs deposition continued until a peak QE was achieved. At this point, the Cs deposition stopped and the QE was monitored to measure the dark lifetime of the photocathode.

After the lifetime measurement, the photocathode was again annealed at 600°C for 6 hours. Subsequently, a CsI layer was grown on the photocathode surface. During the growth, the CsI effusion cell was heated to 500°C, while the photocathode was held at 150°C. The CsI deposition rate was monitored with a QMB until 1 nm was reached. The photocathode then underwent a second activation and lifetime measurement. Following this lifetime measurement, two more cycles of annealing (600°C for 6 hours), activation and lifetime measurement were performed.

RESULTS

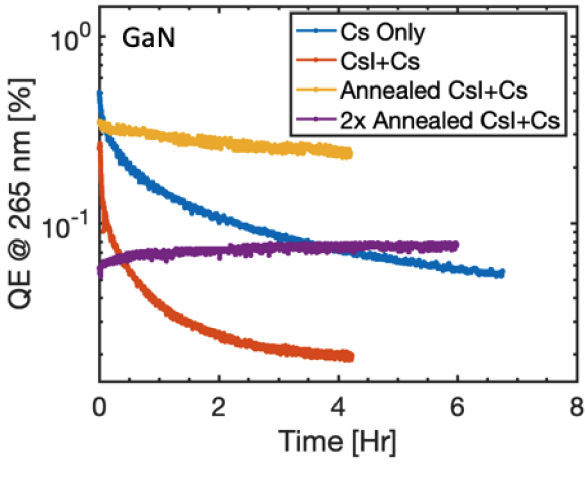
The obtained lifetimes are shown in Fig. 1. In both photocathodes, the initial deposition of 1 nm of CsI on the surface causes a degradation in both QE and lifetime. However, after an additional anneal and activation, the QE is nearly recovered while the 1/e lifetime improves around a factor of 3 for both GaN and GaAs as compared to their initial cesiation. After one more anneal and activation, we observe slightly lower QEs in both cathodes, but significant lifetime improvements. The QE in the GaN photocathode did not degrade over 6 hours of observation and the GaAs photocathode lifetime was improved by a factor of 13 over the initial activation.

ANALYSIS

To investigate the mechanism responsible for the lifetime enhancement, we performed atomic force microscopy (AFM) scans on a GaAs photocathode at each step in the process, as shown in Fig. 2. Figure 2a shows the GaAs sample prior to etching to be very smooth with an RMS roughness of 144 pm, while the sample after etching, shown in Fig. 2b has a slightly increased surface roughness of 285 pm. Note that, in addition to increased roughness, HCl etching has been shown to create a As-rich surface on GaAs [23]. After a 6 hour 600°C anneal, the surface is slightly altered again as shown in Fig. 2c. At this point, after the 1 nm (as measured by the QMB) CsI layer is deposited, the surface of the photocathode features "islands" of CsI, which are several nm tall. These thick domains are likely the cause of poor photocathode performance at this stage, shown in Fig. 2d. Lastly, in Fig. 2e, the quality of the surface is recovered from before the CsI layer deposition.

XPS

Chemical analysis of the surface region of CsI-coated GaAs samples confirmed the presence of CsI and O, as shown by the XPS spectra in Fig. 3a-d. High resolution spectra of the Cs 3d and I 3d transitions were assigned to Cs⁺ and I⁻ in CsI [24]. Unoxidized regions of GaAs gave rise to As 3d photoelectrons at 41.2 eV [25]. There was no distinct sign of GaAs oxidation in the As 3d spectra at



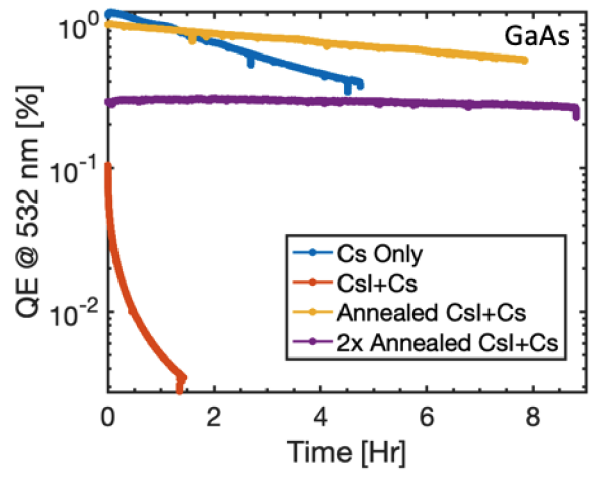


Figure 1: Lifetime measurements of the GaN (top) and GaAs (bottom) photocathodes at various stages. The lifetime after the initial cesiation is shown in blue. An exponential fit yielded a 1/e lifetime of 4.6 Hr and 4.2 Hr respectively for GaN and GaAs. The lifetime after deposition of 1 nm of CsI and subsequent cesiation is shown in red and was fit to a 1/e of 2.9 Hr and 0.6 Hr respectively for GaN and GaAs. After annealing the CsI layer and cesiating again, the lifetime is shown in yellow with a 1/e lifetime of 13.6 Hr and 14.1 Hr respectively in GaN and GaAs. The lifetime after another annealing cycle and cesiation is shown in purple, where in GaAs, the 1/e fit is 77 Hr and in GaN, the QE slightly increases over 6 hours.

45.0 eV transition. From the comparison of spectra taken with normal $(0^{\circ}, \text{ solid lines})$ and glancing $(70^{\circ}, \text{ dotted lines})$ detection, the O species are distributed on the top and bottom of CsI film, with some carboxylates located on the surface

Annealing for 6 hours at 600°C removed all iodine species, as shown by the I 3d spectra in Fig. 3e. Ga 3d high resolution scans in Fig. 3i gave rise to two transitions at 19.3 eV and 20.5 eV, assigned to unoxidized GaAs and Ga oxides, respectively [25]. Some information about the vertical dis-

MC3.T02 Electron Sources 647

doi: 10.18429/JACoW-IPAC2024-MOPR82

Figure 2: AFM scans of a GaAs photocathode at different stages in the CsI enhancement process. A GaAs sample is shown a) as received from the manufacturer, b) after HCl etching, c) after a 6 hour 600°C anneal, d) after the 1 nm (as ready by the QMB) CsI layer is deposited, and e) after another 6 hour 600°C anneal.

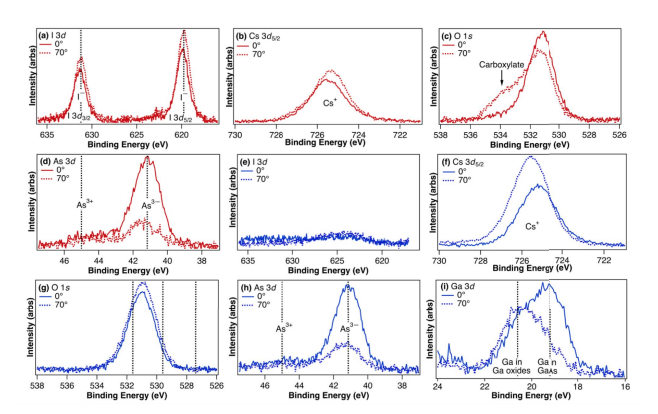


Figure 3: High-resolution X-ray photoelectron spectra of CsI/GaAs (a-d) before and (e-i) after annealing at 600°C observed with normal (0°, solid lines) and glancing (70°, dotted lines) detection displaying the I 3d, Cs $3d_{5/2}$, O 1s, Ga 3d, and As 3d transitions. Vertical dotted lines represent nominal binding energies of (a) I⁻, (g) CsO₂, Cs₂O₂, and Cs_2O , (d, h) As^{3+} and As^{3-} , (i) Ga oxides and GaAs.

tribution of these species could be inferred by comparison of spectra taken at two angles, which showed that Ga oxides were more prevalent in the near-surface region. The identity of the Cs species after annealing could only be inferred indirectly. The presence of metallic Cs could be definitively ruled out by the absence of plasmonic features in the Cs 3d spectra [27], which implied that all Cs was in the +1 oxidation state and thus bound to oxygen, the only observed anion.

The oxidation chemistry of Cs is complex, consisting of peroxides, superoxides, and oxides. The vertical dotted lines in Fig. 3g represent the O 1s binding energies reported in [28] for CsO₂ (531.6 eV), Cs₂O₂ (529.6 eV), and Cs₂O (527.4 eV) [28]. Our XPS analysis suggests that annealing of the CsI-coated GaAs led to desorption of I, presumably as I₂, and the formation of cesium suboxides, such as Cs₂O₂ and CsO₂. We can definitively rule out the production of cesium oxide, Cs₂O. The oxides observed differ from those typically seen in GaAs without CsI [29].

CONCLUSION

It was shown that deposition of a CsI layer can be used to increase the lifetime of both GaN and GaAs photocathodes activated to NEA with cesium. This enhancement effect was investigated with X-ray Photoelectron Spectrosopy (XPS) and Atomic Force Microscopy (AFM).

ACKNOWLEDGEMENTS

The authors thank B.D. Dickensheets, M.W. Olszewski, N. Otto, M.A. Reamon, and B. Vareskic for experimental assistance. This work is supported by U.S. Department of Energy (DOE) grants DE-SC0021002 and DE-SC0023517, and by the U.S. National Science Foundation under Award PHY-1549132, the Center for Bright Beams. The authors acknowledge the use of facilities and instrumentation supported by NSF through the Cornell University Materials Research Science and Engineering Center DMR-1719875.

REFERENCES

ISBN: 978-3-95450-247-9

- D. Xu and et al., "EIC Beam Dynamics Challenges," in Proceedings of the 13th International Particle Accelerator Conference, 2022, WEIXGD1.
- [2] S. Michizono, "The International Linear Collider," *Nature Reviews Physics*, vol. 1, pp. 244–245, 2019.
- [3] "Report of the Community Review of EIC Accelerator R&D for the Office of Nuclear Physics (2017)," 2017. doi:10.2172/1367855
- [4] "Reaching for the Horizon: The 2015 Long Range Plan for Nuclear Science," Tech. Rep., 2015. https://www.osti. gov/biblio/1296778
- [5] "Major Nuclear Physics Facilities for the Next Decade: Report of the NSAC Subcommittee on Scientific Facilities," Tech. Rep., 2013.
- [6] S. Heidrich, K. Aulenbacher, M. Bruker, M. Dehn, and P. Heil, "High-Current Emittance Measurements at MAMI," in *Proc. IPAC'19, Melbourne, Australia, May 2019*, 2019, pp. 4121–4123. doi:10.18429/JACOW-IPAC2019-THPTS009
- [7] P. Adderley *et al.*, "An Overview of How Parity-Violating Electron Scattering Experiments Are Performed at CEBAF," *Nucl. Instrum. Methods Phys. Res. A*, vol. 1046, p. 167710, 2023. doi:10.1016/j.nima.2022.167710
- [8] D. Pierce, R. Celotta, G. Wang, W. Unertl, A. Galejs, and C. Kuyatt, "The GaAs Spin Polarized Electron Source," *Rev. Sci. Instrum.*, vol. 51, pp. 478–499, 1980.
- [9] D. Pierce and F. Meier, "Photoemission of Spin-Polarized Electrons from GaAs," *Phys. Rev. B*, vol. 13, p. 5484, 12 1976. doi:10.1103/PhysRevB.13.5484
- [10] S. Karkare, L. Boulet, A. Singh, R. Hennig, and I. Bazarov, "Ab Initio Studies of Cs on GaAs (100) and (110) Surfaces," *Phys. Rev. B*, vol. 91, p. 035 408, 2015. doi:10.1103/PhysRevB.91.035408
- [11] N. Chanlek et al., "The Degradation of Quantum Efficiency in Negative Electron Affinity GaAs Photocathodes under Gas Exposure," J. Phys. D: Appl. Phys., vol. 47, p. 055 110, 2014.
- [12] T. Wada et al., "Influence of Exposure to CO, CO2 and H2O on the Stability of GaAs Photocathodes," Jpn. J. Appl. Phys., vol. 29, p. 2087, 1990.
- [13] J. Bae, L. Cultrera, P. Digiacomo, and I. Bazarov, "Rugged Spin-Polarized Electron Sources Based on Negative Electron Affinity GaAs Photocathode with Robust Cs₂Te Coating," *Appl. Phys. Lett.*, vol. 112, no. 15, p. 154 101, 2018. doi:10.1063/1.5026701
- [14] L. Cultrera *et al.*, "Long Lifetime Polarized Electron Beam Production from Negative Electron Affinity GaAs Activated with Sb-Cs-O: Trade-Offs between Efficiency, Spin Polarization, and Lifetime," *Phys. Rev. Accel. Beams*, vol. 23, no. 2, p. 023 401, 2020.

- [15] J. Bae et al., "Improved Lifetime of a High Spin Polarization Superlattice Photocathode," J. Appl. Phys., vol. 127, p. 124 901, 2020. doi:10.1063/1.5139674
- [16] J. Bae et al., "Operation of Cs-Sb-O Activated GaAs in a High Voltage DC Electron Gun at High Average Current," AIP Advances, vol. 12, no. 9, p. 095 017, 2022. doi:10.1063/5.0100794
- [17] J. Biswas et al., "High Quantum Efficiency GaAs Photocathodes Activated with Cs, O2, and Te," AIP Advances, vol. 11, no. 2, p. 025 321, 2021. doi:10.1063/5.0026839
- [18] V. Rusetsky et al., "New Spin-Polarized Electron Source Based on Alkali Antimonide Photocathode," Phys. Rev. Lett., vol. 129, p. 166 802, 2022.
- [19] L. Cultrera, "Spin Polarized Electron Beams Production beyond III-V Semiconductors," arXiv, 2022. doi:10.48550/arXiv.2206.15345
- [20] S. J. Levenson et al., Measurement of spin-polarized photoemission from wurtzite and zinc-blende gallium nitride photocathodes, 2024.
- [21] L. Kong, A. G. Joly, T. C. Droubay, and W. P. Hess, "Quantum Efficiency Enhancement in CsI/Metal Photocathodes," *Chemical Physics Letters*, vol. 621, pp. 155–159, 2015. doi:10.1016/j.cplett.2015.01.010
- [22] V. Vlahos, D. Morgan, and J. H. Booske, "Material analysis and characterization of cesium iodide (CsI) coated C fibers for field emission applications," in 2008 IEEE 35th International Conference on Plasma Science, IEEE, 2008, pp. 1–1. doi:10.1109/PLASMA.2008.4590624
- [23] A. Chanda, S. Verma, and C. Jacob, "Etching of GaAs substrates to create As-rich surface," *Bulletin of Materials Science*, vol. 30, no. 6, pp. 561–565, 2007.
- [24] S. W. Gaarenstroom and N. Winograd, "Initial and final state effects in the esca spectra of cadmium and silver oxides," *J. Chem. Phys.*, vol. 67, pp. 3500–3506, 1977.
- [25] C. Y. Su, I. Lindau, P. W. Chye, P. R. Skeath, and W. E. Spicer, "Photoemission studies of the interaction of oxygen with gaas (110)," *Phys. Rev. B*, vol. 25, pp. 4045–4068, 1982.
- [26] J. Balajka *et al.*, "High-affinity adsorption leads to molecularly ordered interfaces on tio2 in air and solution," *Science*, vol. 361, pp. 786–789, 2018.
- [27] J. Hrbek, Y. W. Yang, and J. A. Rodriguez, "Oxidation of cesium multilayers," *Surface Science*, vol. 296, pp. 164–170, 1993
- [28] J. Jupille, P. Dolle, and M. Besancon, "Ionic oxygen species formed in the presence of lithium, potassium and cesium," *Surface Science*, vol. 260, pp. 271–285, 1992.
- [29] C. Y. Su, W. E. Spicer, and I. Lindau, "Photoelectron spectroscopic determination of the structure of (cs,o) activated gaas (110) surfaces," *J. Appl. Phys.*, vol. 54, no. 3, pp. 1413–1422, 1983. doi:10.1063/1.332166

MC3.T02 Electron Sources 649